Journal of Morphology

WILEY

JOURNAL OF morphology

RESEARCH ARTICLE OPEN ACCESS

Middle Ear Mechanics in the Barn Owl

John Peacock[1] | Monica A. Benson[2] | Daniel J. Field[3,4] | Garth M. Spellman[5]

[1]Department of Anatomy and Neurobiology, Northeast Ohio Medical University, Rootstown, Ohio, USA | [2]The Curtis National Hand Center, MedStar Union Memorial Hospital, Baltimore, Maryland, USA | [3]Department of Earth Sciences, University of Cambridge, Cambridge, UK | [4]Museum of Zoology, University of Cambridge, Cambridge, UK | [5]Department of Zoology, Denver Museum of Nature & Science, Denver, Colorado, USA

Correspondence: John Peacock (peacockjohn@outlook.com)

Received: 16 September 2024 | **Revised:** 8 December 2024 | **Accepted:** 10 December 2024

Funding: We thank the Rocky Mountain Raptor Program and Greenwood Wildlife Rehabilitation Center for assistance salvaging the specimens used in this study; Andrea Carrillo and Andrew Doll from DMNS facilitated the loan of specimens; Nathaniel Greene and Daniel Tollin for the use of equipment and for proofreading an earlier manuscript; Joris Dirckx, Pieter Muyshondt, John Rosowski, Hans Thewissen, and Irina Wils for their insightful discussion of the data; all the monks at the Benedictine Abbey of Christ in the Desert for their kind hospitality while preparing this paper. DJF was supported by UK Research and Innovation Future Leaders Fellowship MR/X015130/1. For the purpose of open access, the authors have applied a Creative Commons Attribution (CC BY) licence to any Author Accepted Manuscript version arising.

Keywords: avian | columella | hearing physiology | *Tyto furcata*

ABSTRACT

The barn owl is a common research subject in auditory science due to its exceptional capacity for high frequency hearing and superb sound source localization capabilities. Despite longstanding interest in the auditory performance of barn owls, the function of its middle ear has attracted remarkably little attention. Here, we report the middle ear transfer function measured by laser Doppler vibrometry and direct measurements of inner ear pressures. Our results illustrate that the barn owl middle ear produces a pressure gain between the ear canal and the inner ear vestibule of up to 35 dB, which is comparable to that seen in mammals. The footplate velocity transfer function magnitudes overlap with those measured in other bird species, however the differences in phase between the footplate velocity and the sound pressure stimulus indicate a middle ear group delay that is notably shorter than other birds. This work brings us closer to a more complete understanding of the physiology of hearing in a model organism in auditory science.

1 | Introduction

The barn owl is the most widely distributed owl species on Earth, and is known to possess a wider hearing range than most other birds. While most birds have an upper limit of hearing at ~6000 to 8000 Hz (Dooling 2002), the barn owl's range extends from at least 200 to as high as 14,000 Hz, with the lowest documented sound pressure threshold in all vertebrates of −14.2 dB SPL at 6300 Hz (Dyson, Klump, and Gauger 1998). The barn owl inner ear has the longest basilar papilla of any extant bird species and exhibits an extreme over-representation of hair cells in the 5000−10,000 Hz frequency range (Köppl, Gleich, and Manley 1993). Barn owls also possess several anatomical and physiological adaptations to enhance sound localization ability. These include asymmetrically positioned external ears and a facial ruff to generate acoustical cues (Payne 1971), as well as phase locking capabilities of peripheral auditory nerves that extend to frequencies of up to several kilohertz, which is necessary for encoding the interaural time difference cue to sound location (Köppl 1997). Their exceptional hearing ability has established barn owls as an important model organism in hearing studies (e.g., Bae and Peña 2024; Engler et al. 2020; Grothe 2018; Knudsen 2002; Krumm et al. 2017; Proctor and Konishi 1997; Rucci, Wray, and Edelman 2000; Takahashi 2010; Winkowski and Knudsen 2006)

The barn owl middle ear also exhibits unusual morphological features; for instance, the shape of its columella, with an

extremely large bulbous footplate is unique among birds (Krause 1901; Schwartzkopff 1955; Peacock et al. 2024). Although this morphology has been previously documented, potential functional associations remain unclear, as surprisingly, given the number of published studies on barn owl hearing, the mechanics of the barn owl middle ear remains understudied. Indeed, no direct measurements of middle ear sound transmission have yet been reported for this species.

One way to assess middle ear sound transmission is to measure the columellar footplate velocity transfer function (CVTF), which is the velocity of the footplate (V_{FP}) normalized to the sound pressure in the ear canal. Although data of this kind has been collected from over 40 bird species (Arechvo et al. 2013; Gummer, Smolders, and Klinke Smolders, and Klinke 1989a, 1989b; Muyshondt, Aerts, and Dirckx 2016; Muyshondt et al. 2018; Muyshondt et al. 2016; Peacock et al. 2020; Saunders 1985; Saunders and Johnstone 1972), measurements of CVTF have never been reported for barn owls. To our knowledge, the only reported measurements of barn owl middle ear sound transmission are of tympanic membrane velocity transfer functions (Kettler et al. 2016).

While measurements of CVTF can tell us much about the behavior of the middle ear, this approach has some limitations. Velocity is not a scalar quantity, and the footplate moves in multiple dimensions (Muyshondt et al. 2018; Sim et al. 2010). Particularly at higher frequencies, this motion can become non-piston like and more complex, and a simple measurement of velocity at a single point on the footplate may not fully characterize sound transmission. A more complete means of studying middle ear sound transmission is to measure the resultant inner ear sound pressure directly, and normalize these measurements to the sound pressure in the ear canal. Although this inner ear pressure transfer function (IETF) has been studied in several mammalian species, to our knowledge no similar measurements have been reported for any non-mammal.

In this study, we provide information on the mechanics of the barn owl middle ear. We measured inner ear pressure and columellar footplate motion in response to tones played across the entirety of the barn owl's hearing range. We compare CVTFs and IETFs, the first reported for any bird, and discuss how barn owls compare to other measured species.

2 | Materials and Methods

All barn owls investigated were freshly dead specimens salvaged from the wild; no specimens were killed for this work and collecting complied with all guidelines under requisite regional permits. Four barn owls were acquired as whole frozen carcasses (all *Tyto furcata*), which were allowed to completely thaw before commencing measurements. The use of fresh frozen material has a long history in auditory research (Helmholtz 1868; Politzer 1864; Puria and Rosowski 2012; Von Békésy 1960); Provided that the material has not decayed and is kept moist, frozen material is known to provide a reliable model of middle ear mechanics in the living ear (Ravicz, Merchant, and Rosowski 2000; Rosowski et al. 1990; Von Békésy 1960). None of the specimens showed signs of cranial damage, decomposition, nor any obvious anatomical or physiological abnormalities.

Experiments were performed in a double-walled sound attenuating chamber (IAC Inc. Bronx, NY, USA). Inner ear pressures were measured using small diameter (250 μm) fiber optic pressure probes (FOP-M260-ENCAP, FISO Inc. Canada). Sound stimuli were generated and data collected via a Hammerfall Fireface UCX soundcard (RME, Haimhausen, Germany), and signals were designed using custom-built MATLAB scripts (Mathworks, Natick, MA, USA). Sound was delivered into the ear via a short length of copper tubing and a custom foam eartip which sealed the ear canal. Sound stimuli consisted of 1 s duration tones with logarithmically spaced frequencies between 200 and 14,000 Hz, and the sound pressure level of each stimulus was calibrated in the ear canal using a Bruel and Kjær probe microphone (type 4181, Bruel and Kjær, Denmark). The tip of the probe microphone was placed a few mm from the center of the tympanic membrane, as close as could be achieved without coming into contact with it. We measured each frequency at multiple sound pressure levels ranging from 90 to 110 dB SPL.

To measure the IETF, the inner ear was approached from the medial side after removing the brain. A hole just larger than the diameter of the probe was manually drilled into the vestibule using a fine pick, and the probe was inserted through it. The probe was then sealed in place with alginate impression material (Jeltrate, LD Caulk Co.). To prevent air from entering the inner ear, the endocranium was partially filled with saline and thus hole drilling and probe insertion were performed underwater.

Once these measurements were completed, the pressure probe was removed and the inner ear was completely opened and drained to allow free visual access to the medial (perilymphatic) surface of the footplate for velocity measurements (CVTF). Care was taken to ensure that the bone surrounding the footplate was not disturbed. The vibrations of the footplate were then measured using a laser Doppler vibrometer (Polytec, OFV 5000, Polytec GmbH, Waldbronn, Germany), mounted to a surgical microscope (Zeiss Opmi 1, Carl Zeiss AG, Oberkochen, Germany). Small glass beads were placed on the footplate to enhance the strength of the reflected laser signal. Measurements were made on the center of the footplate with the laser approaching perpendicular to the plane of the footplate as viewed from the perilymphatic side.

We were able to make measurements in six ears from the four owls, however for one ear we were only able to measure CVTF and not IETF. Thus, for the CVTF we have six measurements (six ears from four owls), while for the IETF we have five measurements (five ears from three owls).

Pressure and velocity measurements were not made concurrently for reasons of practicality and to allow for comparison with previous measurements. In barn owls and other birds, simply opening the middle ear cavity is insufficient to view the footplate which is shielded by a bony covering through which the shaft of the columella passes. Exposing the footplate for measurement requires the removal of a considerable amount of additional cranial material, extensively opening the middle ear space, which may significantly change the behavior of the system and risk damaging its delicate structures. Previous studies have opted to keep the middle ear as

intact as possible and instead to open the inner ear (Muyshondt et al. 2018; Muyshondt et al. 2016; Peacock et al. 2020), and we do the same here.

Data analysis was conducted in R (R Core Team 2023). The phylogenetic generalized least squares (PGLS) regression analysis was performed on log-transformed data using the caper package (Orme 2013) with figures plotted using ggplot2 (Wickham 2016).

3 | Results

3.1 | CVTF

The individual CVTF magnitudes (Figure 1A) increased at a rate of around 10 dB/octave to a peak at frequencies between 800 and 1500 Hz, with mean peak value of 2 mm/s/pa at 900 Hz. The magnitude declines following the first peak but then begins to rise again towards a second peak between 4000 and 10,000 Hz (Figure 1). In all cases where high frequency peaks were observed, they were smaller in magnitude than the low frequency peak. The mean phase difference between velocity and stimulus sound pressure (Figure 1B) has an average of 0.1 cycles below 800 Hz, with a value near 0.2 cycles at 1500 Hz, 0 cycles at 2500 Hz and increasingly negative with increasing frequency.

3.2 | IETF

The mean IETF magnitude (Figure 2A) increases from 4 dB at 200 Hz at around 13 dB/octave until it plateaus near 28 dB between 500 and 1500 Hz. The magnitude then declines before rising to reach a second peak of around 35 dB between 5000 and 10,000 Hz. The magnitude then sharply declines above 10,000 Hz. A dip in the transfer function creating two peaks in the IETF is seen in all measurements, and in all cases the high frequency peak was greater in magnitude than the low frequency peak. The mean phase of the inner ear pressure relative

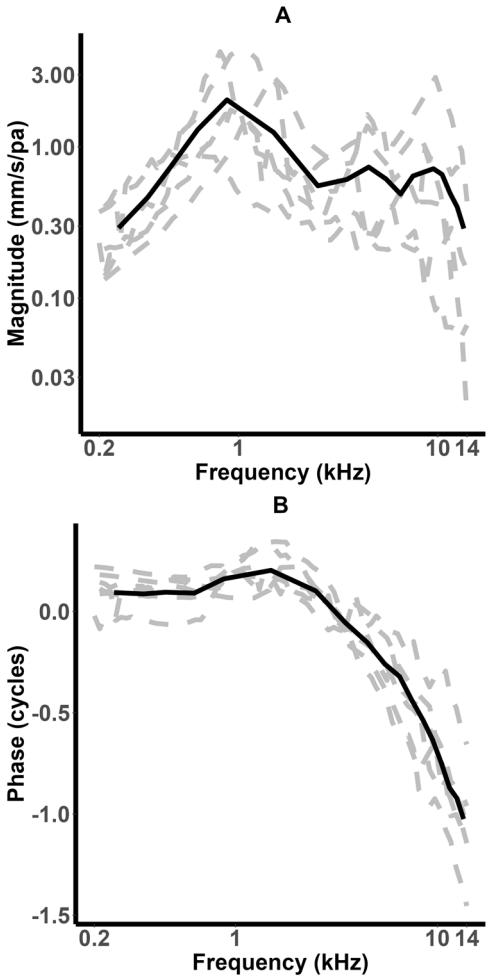

FIGURE 1 | CVTF. Panel (A) shows the velocity of the columellar footplate normalized to the pressure in the ear canal and panel (B) shows the phase of the middle ear velocity relative to the phase of the sound in the ear canal. Gray dashed lines show mean data for individual ears while the black line shows the mean for all measurements. The magnitude is displayed on a dB scale, and the phase is calculated with reference to the phase of the sound in the ear canal.

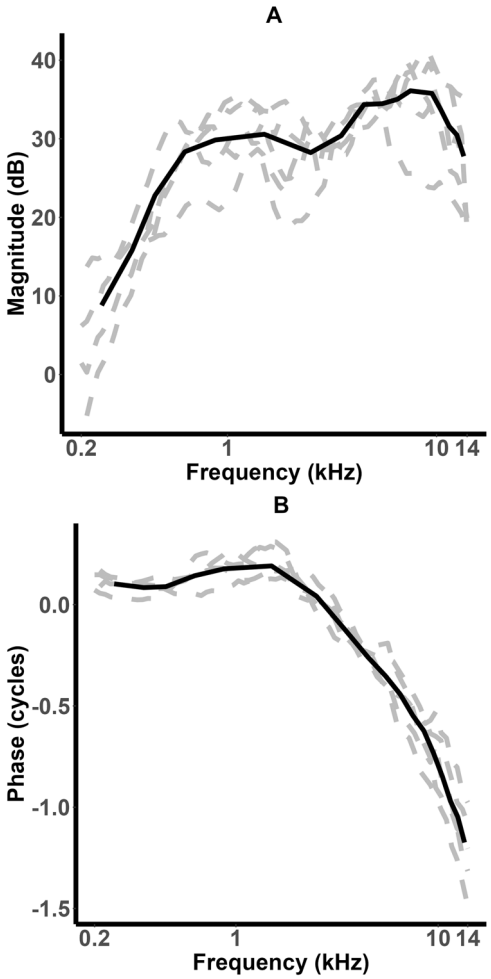

FIGURE 2 | IETF. Panel (A) shows the pressure magnitude in the inner ear normalized to the pressure in the ear canal, and panel (B) shows the phase of the inner pressure relative to the phase of the sound in the ear canal. As with Figure 1, gray dashed lines show mean data for individual ears while the black line shows the mean for all measurements. The magnitude is displayed on a dB scale, and the phase is calculated with reference to the phase of the sound in the ear canals.

to the phase of the sound in the ear canal (Figure 2B) showed a near identical pattern to that shown in Figure 1B for the CVTF. There is a constant phase difference of around 0.1 cycles below 800 Hz, increases to around 0.2 near 1500 Hz, is 0 at 2500 Hz, and becomes increasingly negative at higher frequencies.

3.3 | Comparison of CVTF and IETF

The measured CVTF and IETF are conspicuously different from one another (Figure 3A). The initial slope of the magnitude data is clearly steeper in the pressure data set than in the velocity data set. The first peak in CVTF appears at a lower frequency and is sharper than that seen in the IETF. Above the first peak the velocity and pressure transfer functions diverge, with a 10−12 dB difference appearing between them across frequency. Similar trends in the ratio between IETF and CVTF are observed for all barn owl specimens (Figure 3B), whereby the ratio increases with frequency.

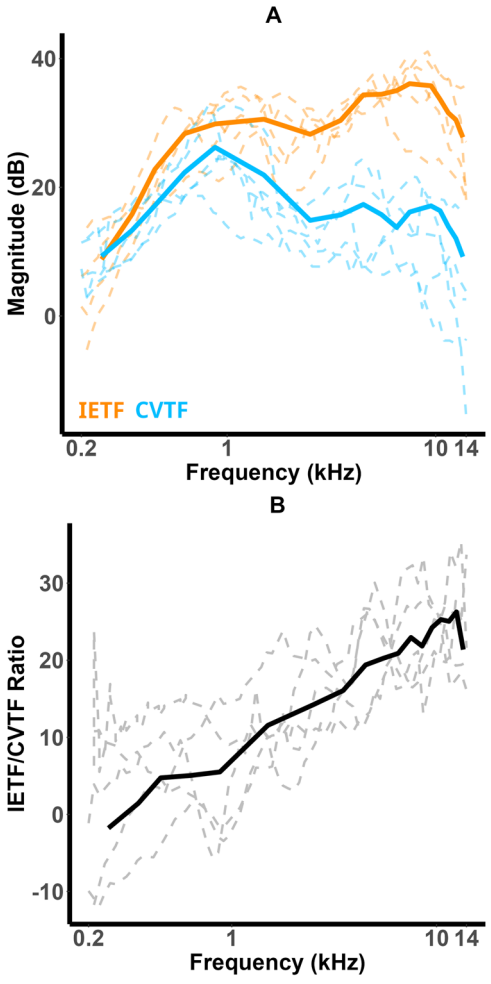

FIGURE 3 | Comparison of CVTF and IETF magnitude. (A) shows the mean values plotted in Figures 1 and 2, the IETF is colored orange and the CVTF is colored blue; the solid lines indicate the means, while the dashed lines are individual animals. The CVTF has been converted to a dB scale with 0 dB set at 10-2 mm/s/pa. The ratio between the IETF and CVTF is shown in (B). In this panel we calculated the ratio for each individual barn owl and each individual is plotted as a separate dashed gray line, while the solid black line shows the mean.

Overall, the difference between the phase of the inner and middle ear transfer functions is small (Figure 4A,B). The mean difference varies between ±0.1 cycles at frequencies less than 1000 Hz and between 0 and −0.15 cycles at higher frequencies (Figure 4B).

3.4 | Comparison of CVTF Between Barn Owls and Other Birds

We compare the CVTF of barn owl with 39 other bird species in Figure 5. A nearly identical low frequency slope in the magnitude (below the first peak) is apparent in all species, followed by a decline in magnitude (Figure 5A). In the barn owl (and a few other species, Peacock et al. 2024) we see a small, gradual increase in magnitude at higher frequencies. The magnitude of the CVTF for the barn owl was greater than most but not all other birds. However, the slope of the phase data when plotted

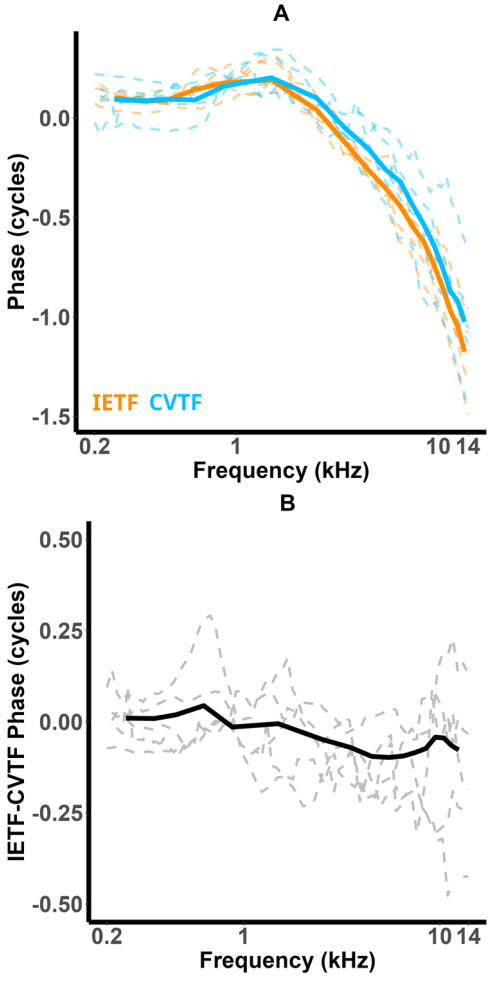

FIGURE 4 | Examination of the differences between the phase of the inner ear and middle ear transfer functions. (A) shows the phase data. As with the previous figure the IETF data are colored orange, the CVTF data are colored blue, and the solid line indicates the mean. These are the same curves as shown in Figures 1 and 2, but plotted together to allow for easier comparison. The difference between the two phases is shown in (B). As before this shows the data calculated for each specimen individually: each individual is plotted as a separate dashed gray line, while the solid black line shows the mean.

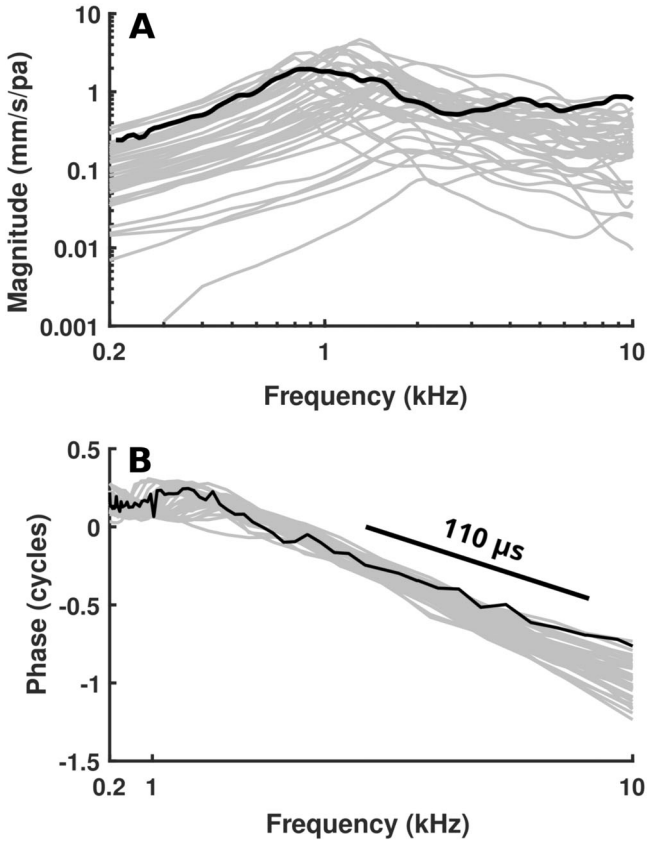

FIGURE 5 | CVTF of the barn owl compared with CVTF measurements from 39 other bird species from Peacock et al. (2020). The black line shows the mean CVTF data for the barn owl. The CVTF magnitude is shown in panel A and the phase in panel B. Note that panel (A) shows frequency on a logarithmic scale, while panel (B) displays this on a linear scale.

on a linear frequency scale (panel B) is notably shallower in the barn owls (Figure 5B). Such a phase vs frequency plot can be used to calculate the middle ear group delay (delay(s) = Δ cycles/Δ cycles per s), and for the barn owl we find a delay of approximately 110 µs (a straight line corresponding to such a delay is shown in Figure 5B). The other avian species, measured in Peacock et al. (2020), show group delays between 134 and 178 µs.

4 | Discussion

4.1 | Middle Ear Pressure Gain in Columellar Ears

Clinical procedures to repair human ears with conductive hearing loss involve reconstructing the three-ossicle mammalian middle ear with a columellar-like prosthesis. Studies in human ears that replaced the incus with a columellar-like partial ossicular replacement prosthesis (PORP) report an overall reduction in inner ear pressures (Dong et al. 2017) and round window displacement (Devèze et al. 2010) at frequencies above 4000 Hz. These results suggest that columellar ears are inherently less efficient at these higher frequencies; however, our barn owl measurements show IETF transfer functions in a similar range

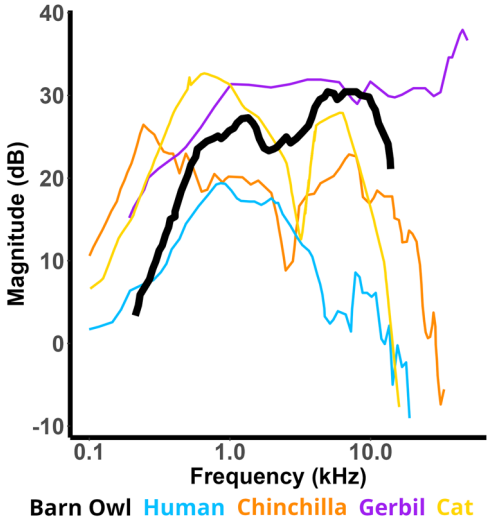

FIGURE 6 | Middle ear pressure gain in the barn owl compared to various mammals. Human data is colored in blue, chinchilla in orange, gerbil in purple, and cat in yellow. The barn owl is the black line.

as various mammals including humans, cats, chinchillas, and gerbils (Décory, Franke, and Dancer 1990; Nakajima et al. 2009; Olson 2001; Ravicz, Slama, and Rosowski 2010, Figure 6).

Our data thus reveal that, despite their morphologically distinctiveness, columellar ears can perform just as well as mammalian ears in terms of pressure gain, including at frequencies above 10 kHz.

It should be remembered that a PORP does not truly replicate the avian middle ear. Simple ossicular replacement prostheses lack the cartilaginous extracolumellae and other elements that contribute to the performance of the avian middle ear system (Köppl 2022). Further study of the avian middle ear, and that of the barn owl in particular, seems warranted as a means to improve hearing outcomes for patients following reconstructive middle ear surgery (see also Manley 2021; Rönnblom et al. 2020).

4.2 | Footplate Velocity Magnitude

While the barn owl is an auditory specialist, with hearing capabilities among the most acute of all tetrapods and an upper frequency limit higher than the majority of non-mammals, the columellar velocity transfer function magnitudes overlap entirely with those of other birds, including at higher frequencies (Figure 5).

A major complication with these measurements is that the columella footplate does not display a simple piston-like motion at all frequencies. Studies in both, mammals and birds, show that while footplate motion is largely piston-like below 1000 Hz, it begins to show rocking motions at higher frequencies which increase in complexity with increasing frequency. This has been described in another owl species, the Boreal Owl (*Aegolius funereus*, Norberg and Boycott 1997). The attachment of the extracolumella from the tympanic ring to the distal end of the bony columella creates an axis of rotation, likely hinging around the infracolumellar process. While this rotation mechanism is different from that found in mammals,

the rotational movement is transferred to the bony columella. Such rotations are further complicated in the barn owl with its uniquely large bulbous footplate that may create an additional rotation axis around the footplate's rim (Schwartzkopff 1955; Krause 1901; Peacock et al. 2024). Further measurements of the columella's three-dimensional motion will be necessary to paint a more complete description of avian middle ear sound transmission.

Although we were unable to find any previous footplate velocity measurements in the barn owl, measurements have been reported of the tympanic membrane (Kettler et al. 2016). These measurements were aimed at assessing the function of interaural canals by measuring umbo velocity from sound played at different locations around the live animal. Overall, they report lower velocities at the umbo than we find for the footplate, and no peak at 1 kHz. Previous measurements have examined the effects of draining the inner ear on umbo velocity, and also compared the V_{FP} and umbo (extrastapedial tip) in the mallard duck (*Anas platyrhynchus*, Muyshondt et al. 2016). After draining the cochlea, this study reported a shift in the initial peak in the umbo velocity transfer function to a higher frequency, overall higher velocities, and the loss of a second smaller high-frequency peak. This study also showed that footplate and umbo velocity in a drained ear track each other closely (with umbo velocity being a few dB higher) until above 5 kHz where the velocities become more similar. Based on this data, higher velocities and some changes in the morphology of the transfer function should be expected in the drained ear. As shown in Figure 5, our velocity measurements are consistent with previous measurements in other bird species.

4.3 | The Relationship between Inner Ear Pressure and Footplate Velocity

Figure 3 shows that measurements of CVTF and IETF have different frequency dependencies, indicating that measurement of CVTF does not describe the frequency dependence of the sound pressure produced in the barn owl's inner ear, especially at the high frequencies.

Sound pressure in the vestibule (P_V) and V_{FP} are related by the cochlear input impedance, Z_C, where: $Z_C = P_V/(V_{FP} \times A_{FP})$ and A_{FP} is a real number describing the area of the footplate. Z_C is a complex quantity having both magnitude and phase angle where the magnitude of Z_C is the ratio of the magnitudes of P_V and ($V_{FP} \times A_{FP}$), and the phase angle of Z_C is the difference of the phases of P_V and V_{FP}. In the case of the barn owl, calculating an exact value for A_{FP}, and thus Z_C, is problematic due to its unusual morphology (see Peacock et al. 2024). However, we can estimate A_{FP} as being between that of a flat surface (1.4 mm^2, producing the largest Z_C magnitude, from Zeyl et al. [2023]) and the curved surface of a hemisphere (with an increase in A_{FP} of ~100%, and the smallest Z_C magnitude). Doing this gives the magnitude of Z_C as between 10^{12} and 10^{13} Pa.s/m^3. This range of impedance magnitude is larger than that reported in other species (see further discussion below).

Our data implies a Z_C magnitude that increases with frequency over the 200 to 10,000 Hz range at around 4–6 dB per octave (Figure 3B). The mean phase difference between IETF and CVTF suggests the angle of Z_C is near 0 at low frequencies and increases with frequency to −0.125 cycles (Figure 4B). The coupling of an increase of Z_C magnitude and a decrease in Z_C phase angle with frequency are inconsistent with any simple mechanical element: The 4–6 dB per octave increase in Z_C magnitude is consistent with an acoustic mass, but a Z_C phase angle of 0 is consistent with a resistance, and an angle of −0.25 is consistent with a spring. Z_C in mammals is often described as resistance like with flat magnitudes with frequency and phase angles near 0 (e.g., [Lynch, Nedzelnitsky, and Peake 1982] in cat; [Nakajima et al. 2009] in human). However, Z_C measurements in chinchillas show a mass-like magnitude growth at high frequencies that is accompanied by a mixed resistance-mass phase angle of near +0.125 cycles at 10 kHz (Ravicz and Rosowski 2013).

A possible explanation for the inconsistency in magnitude and phase is variation in the phase angle measurements. While the individual Z_C magnitudes (Figure 3B) all show a consistent increase with frequency, the individual Z_C phase angle estimates (Figure 4B) vary between ±0.25 periods, with a trend toward phase angles between 0 and −0.25 as frequency increases. It is also possible that errors could have been introduced due to timing delays between the real acoustic stimulus and our measured input signal. This is especially possible since the measurements were made sequentially; as the setup for pressure and velocity measurements were slightly different. Furthermore, the different conditions for the two measurements (inner ear intact for IETF and inner ear drained for CVTF) may have introduced errors into the calculation of Z_C, and additional error may have been introduced due to the draining of the IE.

To our knowledge, the only published measurements of Z_C in any bird were for the Common Ostrich (*Struthio camelus*, Muyshondt, Aerts, and Dirckx 2016). The method of Muyshondt et al. did not involve direct pressure measurements, but they were able to measure with both an intact and drained inner ear. Their measurements also indicated a mass dominated impedance at higher frequencies, with an increasing magnitude similar to ours. However, the impedance magnitude appears to flatten above 2 kHz in the case of the intact ear. These measurements only extended to 4 kHz making it difficult to determine how comparable these measurements are with ours.

Although the hearing ability of the Common Ostrich has not been examined, we expect its highest audible frequency to be around 4-6 kHz based on measurements in other palaeognathous birds such as the Emu (*Dromaius novaehollandiae*, Manley, Köppl, and Yates 1997). Given the distant phylogenetic relationship between the barn owl and the ostrich (Prum et al. 2015), their disparate ear morphologies (Peacock et al. 2024), and pronounced difference in their hearing ability (Manley, Köppl, and Yates 1997), we do not necessarily expect the ostrich ear to behave similarly to that of the barn owl.

In the ostrich, Z_C was found to have a magnitude between 10^9 and 10^{10} Pa.s/m^3, which is smaller than previously measured in mammals: ~10^{10} to 10^{12} Pa.s/m^3. Our measurements indicate that Z_C in the barn owl is not smaller than in mammals, but is

instead greater in magnitude than reported for any other species. As noted by Muyshondt, Aerts and Dirckx (2016), a larger value for Z_C would be expected in smaller animals with smaller IE volumes and footplate areas, although the increase in Z_C from these differences is expected to be smaller than what we observe between the ostrich and barn owl. Previous studies have found differences in relative footplate area among birds (Peacock et al. 2024), with aquatic birds in particular having relatively small footplates. The ostrich is considerably larger than the barn owl, and has a footplate area at least three times larger, however the barn owl was not noted as having a particularly small footplate, and its bulbous nature will actually work to increase its overall area. The barn owl is known to have a greatly elongated cochlear duct but studies of the entire inner ear volume, as well as a clear understanding of what portion of that volume influences footplate motion, are lacking. Regardless, differences in volume alone are unlikely to account for the differences we see in Z_C magnitude. Additional data from other species would be welcome to help characterize and explore this variation.

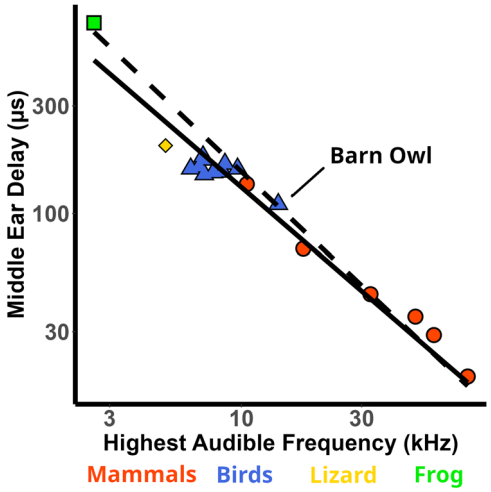

FIGURE 7 | The highest audible frequency at 60 db SPL against middle ear delay. Red circles are mammals, blue triangles are birds, the yellow diamond is the lizard, and the green square is the bullfrog. The results of an ordinary least squares regression are plotted as a dashed line, and the PGLS regression by a solid line.

4.4 | Middle Ear Delay

The 110 µs group delay in the barn owl is the shortest of all previously reported birds, where the average delay was around 150 µs (Peacock et al. 2020). The barn owl delay is shorter than the 138 µs reported in elephants (O'Connell-Rodwell et al. 2024), the 200 µs reported in the bobtail skink (Manley, Yates, and Köppl 1988) and 700 µs reported for female bullfrogs (Van Dijk et al. 2011), but longer than reported for most mammal species commonly used in auditory science: delays of 19 µs have been measured in mice (Dong, Varavva, and Olson 2013), compared with 25–32 µs in gerbils (Olson 1998), 35 µs in guinea pigs (Dancer and Franke 1980), 44 µs in chinchilla (Ravicz and Rosowski 2013), and 56–83 µs in humans (Dong and Olson 2006; Nakajima et al. 2009; O'Connell-Rodwell et al. 2024; O'Connor and Puria 2008).

These species vary in their hearing range: the bullfrog cannot hear much above 2.6 kHz (Megela-Simmons, Moss, and Daniel 1985), while the mouse upper limit is closer to 90 kHz (Koay, Heffner, and Heffner 2002). There does appear to be a trend across species whereby a shorter delay is associated with an increased upper hearing limit (Figure 7). Here, the highest audible frequency is taken at 60 dB SPL from published behavioral audiograms (Dooling 2002; R. Heffner and Heffner 1980; R. Heffner, Heffner, and Masterton 1971; R. Heffner et al. 2020; R. S. Heffner and Heffner 1982, 1991; Jackson, Heffner, and Heffner 1999; Manley 1990; Ryan 1976; Sivian and White 1933).

Both the ordinary least squares (OLS) and PGLS regression analyses of the delay vs highest audible frequency indicate a strong and significant correlation (OLS: $r^2 = 0.96$, $p < 0.00001$, PGLS: $r^2 = 0.87$, $p < 0.00001$). The resulting slope of the OLS and PGLS regression lines were both close to −1 (−1.06 and −0.96 respectively), and the intercept suggests that the delay is between 1.7 or 1.2 times the period of the highest audible frequency. Whether the delay itself plays any role in determining hearing ability is not known. It's likely the delay correlates with the stiffness of the system, and greater stiffness would be expected in ears responsive to higher frequencies; thus, some relationship between these might be expected. However, the reasons for the exact relationship shown in Figure 7 remain to be determined.

The contribution of each component of the middle ear to the delay has not been well studied outside of mammals, but we hypothesize that a considerable part of the delay is contributed by the stiffness of the flexible, cartilaginous extracolumella, with other contributions from stiffnesses in the annular ligament and tympanic membrane.

5 | Conclusion

The barn owl middle ear produces a pressure gain (IETF) between the ear canal and the inner ear vestibule of up to 35 dB, which is comparable to that seen in mammals. However, the overall shape of IETF curves are different to the CVTF curves, and suggests an impedance that is likely mass-dominated across most frequencies. Despite the barn owl middle ear exhibiting unique morphological features and the species' exceptional hearing ability compared to other birds, measurements of CVTF magnitude do not differ substantially from other species. However the delay calculated from the CVTF phase data is shorter than all other birds as well as the single reptile and amphibian species tested, though still considerably longer than those measured in mammals, with the exception of the elephant.

Outstanding questions remain regarding the functional significance of the barn owl's unusual columellar morphology, and the generalizability of the results to other avian species. Future work will shed light on these outstanding questions, and may yield productive avenues for the improvement of human auditory prostheses.

Author Contributions

John Peacock: conceptualization, investigation, formal analysis, writing–review and editing, writing–original draft. **Monica A. Benson:** writing–review and editing, investigation. **Daniel J. Field:** resources, writing–review and editing. **Garth M. Spellman:** resources, writing–review and editing.

Acknowledgments

We thank the Rocky Mountain Raptor Program and Greenwood Wildlife Rehabilitation Center for assistance salvaging the specimens used in this study; Andrea Carrillo and Andrew Doll from DMNS facilitated the loan of specimens; Nathaniel Greene and Daniel Tollin for the use of equipment and for proofreading an earlier manuscript; Joris Dirckx, Pieter Muyshondt, John Rosowski, Hans Thewissen, and Irina Wils for their insightful discussion of the data; all the monks at the Benedictine Abbey of Christ in the Desert for their kind hospitality while preparing this paper. D.J.F. was supported by UK Research and Innovation Future Leaders Fellowship MR/X015130/1. For the purpose of open access, the authors have applied a Creative Commons Attribution (CC BY) licence to any Author Accepted Manuscript version arising.

Conflicts of Interest

The authors declare no conflicts of interest.

Data Availability Statement

All data used to support the findings of this study is included in the article, and can be provided in other formats on request.

References

Arechvo, I., T. Zahnert, M. Bornitz, et al. 2013. "The Ostrich Middle Ear for Developing an Ideal Ossicular Replacement Prosthesis." *European Archives of Oto-Rhino-Laryngology* 270: 37–44.

Bae, A., and J. L. Peña. 2024. "Barn Owls Specialized Sound-Driven Behavior: Lessons in Optimal Processing and Coding By the Auditory System." *Hearing Research* 443: 108952.

Von Békésy, G. 1960. Experiments in Hearing. 745. https://psycnet.apa.org/fulltext/1961-01618-000.pdf.

Dancer, A., and R. Franke. 1980. "Intracochlear Sound Pressure Measurements in Guinea Pigs." *Hearing Research* 2: 191–205.

Décory, L., R. B. Franke, and A. L. Dancer. 1990. "Measurement of the Middle Ear Transfer Function in Cat, Chinchilla and Guinea Pig." In *The Mechanics and Biophysics of Hearing. Lecture Notes in Biomathematics*, edited by P. Dallos, C. D. Geisler, J. W. Matthews, M. A. Ruggero, C. R. Steele, vol 87, 270–277. New York: Springer. https://doi.org/10.1007/978-1-4757-4341-8_33.

Devèze, A., K. Koka, S. Tringali, H. A. Jenkins, and D. J. Tollin. 2010. "Active Middle Ear Implant Application in Case of Stapes Fixation: A Temporal Bone Study." *Otology & Neurotology: Official Publication of the American Otological Society, American Neurotology Society [and] European Academy of Otology and Neurotology* 31: 1027–1034.

Van Dijk, P., M. J. Mason, R. L. M. Schoffelen, P. M. Narins, and S. W. F. Meenderink. 2011. "Mechanics of the Frog Ear." *Hearing Research* 273: 46–58.

Dong, W., and E. S. Olson. 2006. "Middle Ear Forward and Reverse Transmission in Gerbil." *Journal of Neurophysiology* 95: 2951–2961.

Dong, W., Y. Tian, X. Gao, and T. T. Jung. 2017. "Middle-Ear Sound Transmission Under Normal, Damaged, Repaired, and Reconstructed Conditions." *Otology & Neurotology: Official Publication of the American Otological Society, American Neurotology Society [and] European Academy of Otology and Neurotology* 38: 577–584.

Dong, W., P. Varavva, and E. S. Olson. 2013. "Sound Transmission Along the Ossicular Chain in Common Wild-Type Laboratory Mice." *Hearing Research* 301: 27–34.

Dooling, R. 2002. *Avian Hearing and the Avoidance of Wind Turbines*. No. NREL/TP-500-30844. Golden, CO (United States): National Renewable Energy Lab (NREL). https://doi.org/10.2172/15000693.

Dyson, M. L., G. M. Klump, and B. Gauger. 1998. "Absolute Hearing Thresholds and Critical Masking Ratios in the European Barn Owl: A Comparison With Other Owls." *Journal of Comparative Physiology A: Sensory, Neural, and Behavioral Physiology* 182: 695–702.

Engler, S., C. Köppl, G. A. Manley, E. de Kleine, and P. van Dijk. 2020. "Suppression Tuning of Spontaneous Otoacoustic Emissions in the Barn Owl (*Tyto Alba*)." *Hearing Research* 385: 107835.

Grothe, B. 2018. "How the Barn Owl Computes Auditory Space." *Trends in Neurosciences* 41: 115–117.

Gummer, A. W., J. W. Smolders, and R. Klinke. 1989a. "Mechanics of a Single-Ossicle Ear: Ii. The Columella Footplate of the Pigeon." *Hearing Research* 39: 15–25.

Gummer, A. W., J. W. Smolders, and R. Klinke. 1989b. "Mechanics of a Single-Ossicle Ear: I. The Extra-Stapedius of the Pigeon." *Hearing Research* 39: 1–13.

Heffner, R., J. F. Cumming, G. Koay, and H. E. Heffner. 2020. "Hearing in Indian Peafowl (*Pavo Cristatus*): Sensitivity to Infrasound." *Journal of Comparative Physiology A* 206: 899–906.

Heffner, R., and H. Heffner. 1980. "Hearing in the Elephant (*Elephas Maximus*)." *Science* 208: 518–520.

Heffner, R., H. Heffner, and B. Masterton. 1971. "Behavioral Measurements of Absolute and Frequency-Difference Thresholds in Guinea Pig." *Journal of the Acoustical Society of America* 49: 1888–1895.

Heffner, R. S., and H. E. Heffner. 1982. "Hearing in the Elephant (*Elephas Maximus*): Absolute Sensitivity, Frequency Discrimination, and Sound Localization." *Journal of Comparative and Physiological Psychology* 96: 926–944.

Heffner, R. S., and H. E. Heffner. 1991. "Behavioral Hearing Range of the Chinchilla." *Hearing Research* 52: 13–16.

Helmholtz, H. 1868. "Die Mechanik Der Gehörknöchelchen Und Des Trommelfells." *Pflüger, Archiv für die Gesammte Physiologie des Menschen und der Thiere* 1: 1–60.

Jackson, L. L., R. S. Heffner, and H. E. Heffner. 1999. "Free-Field Audiogram of the Japanese Macaque (*Macaca Fuscata*)." *Journal of the Acoustical Society of America* 106: 3017–3023.

Kettler, L., J. Christensen-Dalsgaard, O. N. Larsen, and H. Wagner. 2016. "Low Frequency Eardrum Directionality in the Barn Owl Induced By Sound Transmission Through the Interaural Canal." *Biological Cybernetics* 110: 333–343.

Knudsen, E. I. 2002. "Instructed Learning in the Auditory Localization Pathway of the Barn Owl." *Nature* 417: 322–328.

Koay, G., R. S. Heffner, and H. E. Heffner. 2002. "Behavioral Audiograms of Homozygous Medj Mutant Mice with Sodium Channel Deficiency and Unaffected Controls." *Hearing Research* 171: 111–118.

Köppl, C. 1997. "Phase Locking to High Frequencies in the Auditory Nerve and Cochlear Nucleus Magnocellularis of the Barn Owl, *Tyto Alba*." *Journal of neuroscience* 17: 3312–3321.

Köppl, C. 2022. "Chapter 11—Avian hearing." In *Sturkie's Avian Physiology*, Edited by C. G. Scanes and S. Dridi, (*Seventh Edition*, 159–177. San Diego: Academic Press).

Krause, G. A. J. 1901. *Die Columella der Vögel (Columella auris avium) ihr Bau Und Dessen Einfluss Auf Die Feinhörigkeit: Neue Untersuchungen und*

Beiträge zur comparativen Anatomie des Gehörorganes. Berlin: R. Friedländer & Sohn.

Krumm, B., G. Klump, C. Köppl, and U. Langemann. 2017. "Barn Owls Have Ageless Ears." *Proceedings. Biological Sciences/The Royal Society* 284: 20171584. https://doi.org/10.1098/rspb.2017.1584.

Köppl, C., O. Gleich, and G. A. Manley. 1993. "An Auditory Fovea in the Barn Owl Cochlea." *Journal of Comparative Physiology A* 171: 695–704.

Lynch, T. J., V. Nedzelnitsky, and W. T. Peake. 1982. "Input Impedance of the Cochlea in Cat." *Journal of the Acoustical Society of America* 72: 108–130.

Manley, G. A. 2021. "An Evolutionary Approach to Middle-Ear Prostheses." *Hearing Research* 400: 108144.

Manley, G. A. 1990. "The Bobtail Skink, Tiliqua rugosa." In *Peripheral Hearing Mechanisms in Reptiles and Birds*, Edited by G. A. Manley, 165–190. Berlin, Heidelberg: Springer Berlin Heidelberg.

Manley, G. A., C. Köppl, and G. K. Yates. 1997. "Activity of Primary Auditory Neurons in the Cochlear Ganglion of the Emu *Dromaius novaehollandiae*: Spontaneous Discharge, Frequency Tuning, and Phase Locking." *Journal of the Acoustical Society of America* 101: 1560–1573.

Manley, G. A., G. K. Yates, and C. Köppl. 1988. "Auditory Peripheral Tuning: Evidence for a Simple Resonance Phenomenon in the Lizard Tiliqua." *Hearing Research* 33: 181–189.

Megela-Simmons, A., C. F. Moss, and K. M. Daniel. 1985. "Behavioral Audiograms of the Bullfrog (Rana Catesbeiana) and the Green Tree Frog (*Hyla Cinerea*)." *Journal of the Acoustical Society of America* 78: 1236–1244.

Muyshondt, P. G. G., P. Aerts, and J. J. J. Dirckx. 2016. "Acoustic Input Impedance of the Avian Inner Ear Measured in Ostrich (*Struthio camelus*)." *Hearing Research* 339: 175–183.

Muyshondt, P. G. G., R. Claes, P. Aerts, and J. J. J. Dirckx. 2018. "Quasi-Static and Dynamic Motions of the Columellar Footplate in Ostrich (*Struthio camelus*) Measured Ex Vivo." *Hearing Research* 357: 10–24.

Muyshondt, P. G. G., J. A. M. Soons, D. De Greef, F. Pires, P. Aerts, and J. J. J. Dirckx. 2016. "A Single-Ossicle Ear: Acoustic Response and Mechanical Properties Measured in Duck." *Hearing Research* 340: 35–42.

Nakajima, H. H., W. Dong, E. S. Olson, S. N. Merchant, M. E. Ravicz, and J. J. Rosowski. 2009. "Differential Intracochlear Sound Pressure Measurements in Normal Human Temporal Bones." *Journal of the Association for Research in Otolaryngology* 10: 23–36.

Norberg, R. Å., and B. B. Boycott. 1997. "Skull Asymmetry, Ear Structure and Function, and Auditory Localization in Tengmalm's Owl, *Aegolius funereus* (Linné)." *Philosophical Transactions of the Royal Society of London, Series B: Biological Sciences* 282: 325–410.

O'Connell-Rodwell, C. E., J. L. Berezin, A. Dharmarajan, et al. 2024. "The Impact of Size on Middle-Ear Sound Transmission in Elephants, the Largest Terrestrial Mammal." *PLoS One* 19: e0298535.

O'Connor, K. N., and S. Puria. 2008. "Middle-Ear Circuit Model Parameters Based on a Population of Human Ears." *Journal of the Acoustical Society of America* 123: 197–211.

Olson, E. S. 1998. "Observing Middle and Inner Ear Mechanics With Novel Intracochlear Pressure Sensors." *Journal of the Acoustical Society of America* 103: 3445–3463.

Olson, E. S. 2001. "Intracochlear Pressure Measurements Related to Cochlear Tuning." *Journal of the Acoustical Society of America* 110: 349–367.

Orme, D. 2013. The Caper Package: Comparative Analysis of Phylogenetics and Evolution in R.

Payne, R. S. 1971. "Acoustic Location of Prey By Barn Owls (*Tyto Alba*)." *Journal of Experimental Biology* 54: 535–573.

Peacock, J., G. M. Spellman, D. J. Field, M. J. Mason, and G. Mayr. 2024. "Comparative Morphology of the Avian Bony Columella." *The Anatomical Record* 307: 1735–1763.

Peacock, J., G. M. Spellman, D. J. Tollin, and N. T. Greene. 2020. "A Comparative Study of Avian Middle Ear Mechanics." *Hearing Research* 395: 108043.

Politzer, A. 1864. "Untersuchungen Über Schallfortpflanzung Und Schallleitung Im Gehörorgane Im Gesunden Und Kranken Zustande." *Archiv für Ohrenheilkunde* 1: 59–73.

Proctor, L., and M. Konishi. 1997. "Representation of Sound Localization Cues in the Auditory Thalamus of the Barn Owl." *Proceedings of the National Academy of Sciences* 94: 10421–10425.

Prum, R. O., J. S. Berv, A. Dornburg, et al. 2015. "A Comprehensive Phylogeny of Birds (Aves) Using Targeted Next-Generation Dna Sequencing." *Nature* 526: 569–573.

Puria, S., and J. J. Rosowski. 2012. "Békésy's Contributions to Our Present Understanding of Sound Conduction to the Inner Ear." *Hearing Research* 293: 21–30.

R Core Team. 2023. R: A Language and Environment for Statistical Computing. R Foundation for Statistical Computing. https://www.R-project.org.

Ravicz, M. E., S. N. Merchant, and J. J. Rosowski. 2000. "Effect of Freezing and Thawing on Stapes-Cochlear Input Impedance in Human Temporal Bones." *Hearing Research* 150: 215–224.

Ravicz, M. E., and J. J. Rosowski. 2013. "Middle-Ear Velocity Transfer Function, Cochlear Input Immittance, and Middle-Ear Efficiency in Chinchilla." *The Journal of the Acoustical Society of America* 134: 2852–2865.

Ravicz, M. E., M. C. C. Slama, and J. J. Rosowski. 2010. "Middle-Ear Pressure Gain and Cochlear Partition Differential Pressure in Chinchilla." *Hearing Research* 263: 16–25.

Rönnblom, A., K. Gladiné, A. Niklasson, M. von Unge, J. Dirckx, and K. Tano. 2020. "A New, Promising Experimental Ossicular Prosthesis: A Human Temporal Bone Study With Laser Doppler Vibrometry." *Otology & Neurotology: Official Publication of the American Otological Society, American Neurotology Society [and] European Academy of Otology and Neurotology* 41: 537–544.

Rosowski, J. J., P. J. Davis, K. M. Donahue, S. N. Merchant, and M. D. Coltrera. 1990. "Cadaver Middle Ears As Models for Living Ears: Comparisons of Middle Ear Input Immittance." *Annals of Otology, Rhinology, & Laryngology* 99: 403–412.

Rucci, M., J. Wray, and G. M. Edelman. 2000. "Robust Localization of Auditory and Visual Targets in a Robotic Barn Owl." *Robotics and Autonomous Systems* 30: 181–193.

Ryan, A. 1976. "Hearing Sensitivity of the Mongolian Gerbil, Meriones Unguiculatis." *Journal of the Acoustical Society of America* 59: 1222–1226.

Saunders, J. C. 1985. "Auditory Structure and Function in the Bird Middle Ear: An Evaluation By Sem and Capacitive Probe." *Hearing Research* 18: 253–268.

Saunders, J. C., and B. M. Johnstone. 1972. "A Comparative Analysis of Middle-Ear Function in Non-Mammalian Vertebrates." *Acta Oto-laryngologica* 73: 353–361.

Schwartzkopff, J. 1955. "On the Hearing of Birds." *The Auk* 72: 340–347.

Sim, J. H., M. Chatzimichalis, M. Lauxmann, C. Röösli, A. Eiber, and A. M. Huber. 2010. "Complex Stapes Motions in Human Ears." *Journal of the Association for Research in Otolaryngology* 11: 329–341.

Sivian, L. J., and S. D. White. 1933. "Minimum Audible Sound Fields." *Journal of the Acoustical Society of America* 5: 65.

Takahashi, T. T. 2010. "How the Owl Tracks Its Prey—II." *Journal of Experimental Biology* 213: 3399–3408.

Wickham, H. 2016. "Data Analysis." In *ggplot2: Elegant Graphics for Data Analysis*, Edited by H. Wickham, 189–201. Cham: Springer International Publishing.

Winkowski, D. E., and E. I. Knudsen. 2006. "Top-Down Gain Control of the Auditory Space Map By Gaze Control Circuitry in the Barn Owl." *Nature* 439: 336–339.

Zeyl, J. N., E. P. Snelling, R. Joo, and S. Clusella-Trullas. 2023. Scaling of ear morphology across 127 bird species and its implications for hearing performance. *Hearing Research* 428: 108679.